Cation−π−Anion Interaction: A Theoretical Investigation of the Role of Induction Energies

Dongwook Kim,[†,‡] Eun Cheol Lee,[†] Kwang S. Kim,*[,†] and P. Tarakeshwar*[,§]

Center for Superfunctional Materials, Department of Chemistry, Pohang University of Science and Technology, San 31, Hyojadong, Pohang 790-784, Korea, School of Computational Sciences, Korea Institute for Advanced Study, 207-43, Cheongnyangni-2-dong, Dongdaemun-gu, Seoul 130-722, Korea

Received: May 1, 2007; In Final Form: June 8, 2007

Cation−π and the corresponding anion−π interactions have in general been investigated as binary complexes despite their association with counterions. However, a recent study of the ammonia channel highlights the important but overlooked role of anions in cation−π interactions. In an effort to examine the structural and energetic consequences of the presence of counterions, we have carried out detailed ab initio calculations on some model cation−π−anion ternary complexes and evaluated the nonpair potential terms, three-body contributions, and attractive and repulsive energy components of the interaction energy. The presence of the anion in the vicinity of the π system leads to a large redistribution of electron density and hence leads to an inductive stabilization. The resulting electronic and geometrical changes have important consequences in both chemical and biological systems. Compared to cation−π−anion ternary complexes, the magnitude of the cation−π interaction in π−cation−anion ternary complexes is markedly lower because of charge transfer from the anion to the cation.

1. Introduction

Investigations of noncovalent intermolecular interactions have in general involved hydrogen bonds, hydrophobic interactions, and ionic interactions. However, in the recent past, intermolecular interactions involving π systems have attracted a lot of interest because of their utility in molecular recognition, rational material design, creation of molecular materials with desirable physical properties, elucidation of enzymatic reaction mechanisms, understanding biomolecular structures, etc.[1−5] Nonetheless, it has also been realized that the relevance of these intermolecular interactions stems from a delicate balance of competing and cooperative interactions.[6−11]

Generally, theoretical investigations of intermolecular interactions have mostly focused their attention on binary complexes. However, most intermolecular interactions involve ternary complexes, as can be noted from extensive studies on the adsorption and distribution of ions at the interface of water and crown ethers,[12] the relative arrangement of ions at the vapor/liquid interface of atmospheric particle surfaces,[13] etc. On a similar note in biological systems, a lot of interest has been evinced on the structure determining roles of noncovalent interactions in the presence of competing forces.[14]

Against this background, we thought it would be of interest to extend our extensive work on binary systems containing π systems to ternary complexes involving π systems. It is pertinent to note that electrostatic interactions between the anions and cations have been implicated in facilitating cation−π interactions in the solid and liquid states.[15−19] The recently determined X-ray structure of the ammonia channel, wherein a negatively charged amino acid (Asp^{160}) plays a crucial role in governing the ammonium cation-attracting capabilities of some of the aromatic amino acid residues close to the channel, provided additional impetus to this investigation.[20] It is particularly interesting to note that the hydrophobic aromatic residue (Trp^{148}) shields the negatively charged (Asp^{160}) residue from the solvent. Therefore, solvent effects would not have a significant influence on the cation−π−anion interactions prevalent in these systems.

Unlike cation−π interactions, which have been the focus of extensive theoretical investigations, there are relatively few studies on interactions involving anions and π systems.[21−26] This is because of the fact that interactions involving anions and π systems are predominantly dominated by dispersion energies.[25] Therefore, an accurate theoretical description of these interactions requires both large basis sets to describe the diffuse nature of the anion and π systems and the explicit inclusion of electron correlation.

We employed a combination of different theoretical methods to obtain a comprehensive insight into the nature of interaction of ternary cation−π−anion complexes. We initially carried out conventional supermolecular (SM) calculations on ternary complexes containing benzene, cations (Li^+, Na^+, K^+, NH_4^+), and anions (F^-, Cl^-, Br^-) to obtain the optimized geometries and interaction energies. The interaction energies were then decomposed to obtain the two-body, three-body, and relaxation energy contributions.[27−30] We also carried out perturbational calculations on the optimized geometries to obtain the magnitudes of the individual attractive and repulsive energy terms.[31−33] An analysis of the electron densities of these ternary complexes was carried out to obtain more insight into the interactions, viz., geometries and the magnitude of the individual interaction energies.[34−37]

2. Methods

Theoretical investigations of noncovalent intermolecular interactions can be carried out using either the SM variational

* Corresponding authors. E-mail: K.S.K., kim@postech.ac.kr; P.T., tara@kias.re.kr.
† Pohang University of Science and Technology.
‡ Present address: School of Chemistry and Biochemistry, Georgia Institute of Technology, Atlanta, GA, 30332-0400.
§ Korea Institute for Advanced Study.

10.1021/jp073337x CCC: $37.00
Published on Web 07/26/2007

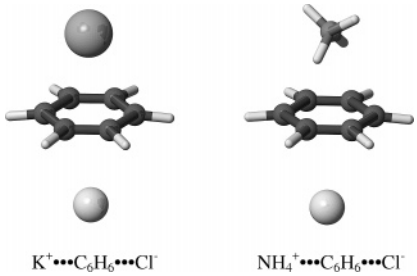

Figure 1. Representative structures of (a) the complex of K^+, benzene, and Cl^-, and (b) the complex of NH_4^+, benzene, and Cl^- with K^+, NH_4^+, and Cl^- fixed along the C_6 axis of benzene.

method or perturbational methods.[38] Although the SM method is conceptually and computationally simple, it does not provide a clear picture of the individual interactions. On the other hand, perturbational methods compute the interaction energy directly as a sum of electrostatic, exchange, induction, and dispersion contributions; hence, a physical interpretation of the interactions between the complex monomers can be obtained.

2.1. Supermolecular Calculations. All the SM calculations were carried out at the second-order Møller−Plesset (MP2) level of theory using the 6-31+G* basis set. All electrons were explicitly correlated in MP2 calculations. The optimizations were carried out on structures, wherein the cation (Li^+, Na^+, K^+) and anion (F^-, Cl^-, Br^-) were aligned along the C_6 axis of the π system (benzene). In the case of complexes involving NH_4^+, the nitrogen atom of the ammonium cation and the anion were aligned along the C_6 axis. Two representative optimized structures ($K^+\cdots C_6H_6\cdots Cl^-$ and $NH_4^+\cdots C_6H_6\cdots Cl^-$) are shown in Figure 1. Basis set superposition error (BSSE) corrections for all these complexes were carried out using the counterpoise (CP) method of Boys and Bernardi.[39]

The natural bond orbital (NBO) analysis method has been employed to evaluate the atomic charges in all the complexes,[40] because unlike most other charge partitioning schemes, it is unaffected by the presence of diffuse functions in the basis set. The NBO charges reported in this study have been calculated using the densities obtained at the MP2 level.

All the SM calculations were carried out using the GAUSSIAN suite of programs,[41] and the electron density analysis was carried out using the GAMESS suite of programs.[42]

2.2. Symmetry-Adapted Perturbation Theory Calculations. In this study, the perturbational calculations were carried out using the optimized geometries of all the complexes that were obtained from SM calculations. The perturbational calculations of the binary systems $M^+\cdots(\pi\cdots X^-)$, $(M^+\cdots\pi)\cdots X^-$ were performed on the optimized geometries of the corresponding ternary complexes ($M^+\cdots\pi\cdots X^-$).

The symmetry adapted perturbation theory (SAPT) interaction energy up to the second order, E_{int}, is given by

$$E_{int} = E_{es}^{(1)} + E_{exch}^{(1)} + E_{ind}^{(2)} + E_{exch-ind}^{(2)} + E_{disp}^{(2)} + E_{exch-disp}^{(2)} + \delta_{int}^{HF} = E_{es} + E_{exch} + E_{ind} + E_{disp}$$
$$(E_{exch} = E_{exch}^{(1)} + E_{exch-ind}^{(2)} + E_{exch-disp}^{(2)} + \delta_{int}^{HF}) \qquad (1)$$

where $E_{es}^{(1)}$ is the electrostatic energy of monomers with the unperturbed electron distributions, $E_{exch}^{(1)}$ is their first-order valence repulsion energy due to the Pauli exclusion principle, $E_{ind}^{(2)}$ stands for the second-order energy gain resulting from the induction interaction, $E_{exch-ind}^{(2)}$ represents the repulsion change due to the electronic cloud deformation, $E_{disp}^{(2)}$ is the second-order dispersion energy, $E_{exch-disp}^{(2)}$ denotes the second-order correction for a coupling between the exchange repulsion and the dispersion interaction, and δ_{int}^{HF} includes the higher order induction and exchange corrections. Because the BSSE correction is explicitly included in evaluating the SAPT interaction energies, the BSSE corrected supermolecular interaction energy (E_{tot}^{SM}) would be similar to the SAPT interaction energy, E_{int}.

Given the size of the systems and the level of theory employed in this study, it was not feasible to evaluate the computationally demanding higher order components using the basis sets employed in the SM calculations. Therefore, we used the 6-31G* basis set and restricted the order of energy components ($n \leq 2$). Accordingly, one should expect a slight deviation of the total interaction energies evaluated using SAPT and SM calculations. This, however, does not affect our conclusions based on the magnitude of the individual interaction energy components, as was shown in recent papers.[43−45] A detailed description of SAPT and some of its applications can be found in some recent references.[31−33,46−48]

2.3. Many-Body Energy Decomposition. One can also analyze the interaction energies of these ternary complexes in terms of the contributions of the two-body and three-body contributions. Thus, the total energy of the ternary complex is analyzed in terms of the contributions of the two-body (E_{ij}), three-body (E_{ijk}), and relaxation (E_{rlx}) terms.[27−30]

TABLE 1: MP2/6-31+G* Interaction Energies and Intermolecular Distances of the Binary $M^+\cdots C_6H_6$ and $C_6H_6\cdots X^-$ complexes[a]

	E_{tot}^{SM}	$R_\perp$
	$X^-\cdots C_6H_6$	
F^-	2.87	3.46
Cl^-	2.69	3.79
Br^-	2.14	3.89
	$M^+\cdots C_6H_6$	
Li^+	−34.60	1.91
Na^+	−22.14	2.40
K^+	−15.47	2.90
NH_4^+	−15.74	2.99

[a] E_{tot}^{SM} is the BSSE-corrected binding energy in kcal/mol. $R_\perp$ (Å) denotes the perpendicular distance from the center of the hexagonal ring of the benzene molecule to the ion (the ion position of NH_4^+ corresponds to the nitrogen atom).

3. Results and Discussion

We initially carried out calculations on the binary complexes of benzene with different cations and halide ions. Expectedly, the negatively charged halide anions exhibit a repulsive interaction and the positive charged cations exhibit an attractive interaction with benzene (Table 1). In the case of interactions involving the anions, the interaction energy is less repulsive for the larger sized anions. On the other hand, the interaction energy is less attractive for the larger sized cations.[24,25]

It should be noted that the most stable gas-phase structure of the ternary system would be the ($\pi\cdots M^+\cdots X^-$) complex. However, we do not consider this structure because most ion pairs would dissociate in polar solvents and moreover in the process of forming a contact ion pair with an anion, the positive charge of the cation is dramatically reduced. Thus, in the case of the ternary benzene$\cdots NH_4^+\cdots Cl^-$ complex, the ion pair transforms itself into the more stable and neutral benzene$\cdots NH_3\cdots HCl$ complex. In this process, the stabilization of 16 kcal/mol accruing from the cation−π interaction of the benzene and the ammonium cation is drastically reduced to 2.0 kcal/mol

TABLE 2: Calculated (MP2/6-31+G*) Intermolecular Energies and Intermolecular Distances of All the $M^+\cdots C_6H_6\cdots X^-$ Complexes[a]

	E_{ij}[b]								
X^-	$M^+\cdots\pi$	$M^+\cdots X^-$	$\pi\cdots X^-$	ΣE_{ij}	E_{ijk}[b]	E_{rlx}[c]	E_{tot}^{SM}	$R_{M^+\cdots\pi}$	$R_{\pi\cdots X^-}$
				$M^+ = Li^+$					
F^-	−33.64	−81.22	9.45	−105.41	−8.48	0.37	−113.52	1.79	2.42
Cl^-	−33.96	−72.04	8.02	−97.98	−6.56	0.54	−104.00	1.81	3.00
Br^-	−34.06	−70.37	6.67	−97.76	−5.83	0.54	−103.05	1.81	3.15
				$M^+ = Na^+$					
F^-	−21.24	−71.80	7.92	−85.13	−8.56	0.89	−92.79	2.25	2.47
Cl^-	−21.60	−64.36	6.85	−79.10	−6.81	1.05	−84.87	2.27	3.04
Br^-	−21.69	−62.97	5.68	−78.95	−6.29	1.03	−84.22	2.28	3.19
				$M^+ = K^+$					
F^-	−14.75	−64.66	7.03	−72.38	−7.71	1.02	−79.07	2.71	2.52
Cl^-	−15.14	−58.43	6.27	−67.30	−6.12	1.22	−72.20	2.73	3.08
Br^-	−15.17	−57.21	5.21	−67.18	−5.71	1.19	−71.69	2.74	3.22
				$M^+ = NH_4^+$					
F^-	−15.98	−64.67	7.12	−73.53	−9.45	2.13	−80.85	2.79[d]	2.51
Cl^-	−16.18	−58.30	6.18	−68.31	−7.46	2.10	−73.67	2.80[d]	3.08
Br^-	−16.20	−57.04	5.05	−68.19	−6.95	2.00	−73.15	2.81[d]	3.23
Cl^-[e]	−18.67	−59.17	4.91	−72.93	−12.58	1.81	−83.70	2.73[d]	2.98

[a] All energies (in kcal/mol) are BSSE-corrected. [b] E_{ij} and E_{ijk} are the two-body and three-body interaction energies. [c] E_{rlx} is the total relaxation energy which is expressed as the difference of the isolated and complexed monomer energies constituting the ternary complex. [d] When M^+ is NH_4^+, $R_{M^+\cdots\pi}$ is defined as a distance between center of benzene ring and N atom of NH_4^+. [e] MP2/aug-cc-pVDZ results.

(interaction energy of the benzene−NH_3 complex).[49] A smaller but still significant change could be noted also in the case of the benzene$\cdots NH_4^+\cdots HCOO^-$ complex.[18]

In light of the above, all our calculations of ternary complexes have been carried out on the ($M^+\cdots\pi\cdots X^-$) structural motif. Apart from understanding the role of the π system, calculations on such a structure would also help understand the roles of both the anion and cation in modulating the corresponding cation−π and anion−π interactions.

In Table 2, the intermolecular distances between the anion and C_6H_6 ($R_{\pi\cdots X^-}$) and between the cation and C_6H_6 ($R_{M^+\cdots\pi}$), and the corresponding two-body, three-body, and relaxation energies of these $M^+\cdots X^-$ complexes are listed. It can be seen that the presence of the counterion on the other side of the π system leads to the anion or cation being pulled much closer to the benzene molecule. However, this effect is more perceptible in the case of the anion−π interaction. Thus, in the presence of cations, the anions are pulled much closer to the benzene atom, with the decrease in $R_{\pi\cdots X^-}$ ranging between 0.6 and 1.0 Å.

The energies listed in Table 2 indicate that the two-body cation−π and the electrostatic cation−anion interactions are the main contributors to the total interaction energy. Expectedly, the anion−π interactions are repulsive in the equilibrium geometries of the corresponding ternary complexes. It is interesting to note in Table 2, that the magnitude of the three-body contributions to the total interaction energy is slightly larger than that of the repulsive anion−π interaction energy in case of the Na^+, K^+ and NH_4^+ cation containing ternary complexes. To ascertain the veracity of this observation, we carried out calculations on the $NH_4^+\pi\cdots Cl^-$ complex using the aug-cc-pVDZ basis set at the MP2 level. It can clearly be seen from Table 2, that the MP2/aug-cc-pVDZ results reinforce the MP2/6-31+G* observations with the difference in magnitudes being vastly enhanced.

It is therefore interesting to examine the underlying factors responsible for the enhancement of the three-body interaction energies vis-a-vis the corresponding two-body interaction energies. Although it might be possible that the repulsive anion−π interaction is being stabilized by electrostatic interactions due to the presence of the cation, an analysis of the charges (Table 3) did not provide any indications of the same.

The energy decompositions of two-body systems have been well documented. However, the same cannot be said for three-body systems. We, therefore, in Tables 4 and 5, examine the ternary ($M^+\cdots\pi\cdots X^-$) complex in terms of intermolecular interactions involving the binary systems {($M^+\cdots\pi$)$\cdots X^-$, ($\pi\cdots X^-$), ($M^+\cdots X^-$), $M^+\cdots(\pi\cdots X^-)$ and ($\pi\cdots M^+$)}. For the sake of brevity, the numbers have been given only for the {$Na^+\cdots\pi\cdots X^-$, X = F, Cl, Br} and {$M^+\cdots\pi\cdots Cl^-$, M = Li, K, NH_4} complexes. It can be noted from Table 4 that the magnitude of dispersion energies is nearly the same in the ($M^+\cdots\pi$)$\cdots X^-$ and ($\pi\cdots X^-$) complexes. A similar observation can be made in the case of the $M^+\cdots(\pi\cdots X^-)$ and ($M^+\cdots\pi$) complexes in Table 5. Though the increased electrostatic interactions in the binary systems containing both the anion and the cation can be attributed to the Coulombic interaction between the cation and the anion (Tables 4 and 5), the increase in the magnitude of the attractive induction energies and repulsive exchange energies is interesting. One plausible explanation is that the presence of the cation and the anion on the opposite sides with respect to the π system enhances the polarization of the π system.

Before we discuss this issue in terms of the electron density difference maps, we think it would be useful to examine the energetic details of the $NH_4^+\cdots\pi\cdots Cl^-$ complex in terms of the corresponding binary systems ($M^+\cdots X^-$), ($M^+\cdots\pi$), ($X^-\cdots\pi$), $M^+\cdots(\pi\cdots X^-)$, ($M^+\cdots\pi$)$\cdots X^-$, ($M^+\cdots X^-$)$\cdots\pi$ at the aug-cc-pVDZ level (Table 6). The sum of two-body interaction energies can be given as ΣE_{ij} (−74.80 kcal/mol) = $E_{M^+\cdots X^-}$ (−59.86 kcal/mol) + $E_{M^+\cdots\pi}$ (−18.54 kcal/mol) + $E_{\pi\cdots X^-}$ (3.60 kcal/mol). For $E_{M^+\cdots X^-}$, the electrostatic energy E_{es} (−58.85 kcal/mol) is the major attractive energy component, whereas for both $E_{M^+\cdots\pi}$ and $E_{\pi\cdots X^-}$, the induction energies E_{ind} (−22.29 and −24.54 kcal/mol) are the dominating contributors to the total two-body attractive energy. It is interesting to examine the modulation of the energies, when we add the third molecule/ion to the binary systems discussed above, viz. $M^+\cdots(\pi\cdots X^-)$, ($M^+\cdots\pi$)$\cdots X^-$, and ($M^+\cdots X^-$)$\cdots\pi$. When the cation (M^+) interacts with the ($\pi\cdots X^-$) system, the total interaction energy is larger in magnitude than the sum of the corresponding binary interaction energies, $E_{M^+\cdots X^-}$ and $E_{\pi\cdots X^-}$. When we analyze this difference in terms of individual interaction energy components, one notes that the induction energy (E_{ind} = −4.62 kcal/mol) predominantly results from the charge reorganization of the π system in the ternary complex. The magnitude of the electrostatic energy (E_{es} = −10.14 kcal/mol) reflects the changes in the magnitudes of the charge densities as a result of the reorganization. A similar observation can be made, when the anion (X^-) interacts with the binary ($\pi\cdots M^+$) system.

Given this background, it would be interesting to examine the modulation of each of these interaction energy components when the cation or anion is brought close to the corresponding anion−π or cation−π complex. Therefore we carried out DFT-SAPT calculations using the aug-cc-pVDZ basis set on both the $Na^+\cdots\pi\cdots Cl^-$ and $NH_4^+\cdots\pi\cdots Cl^-$ complexes.[50] It should be reiterated that both conventional SAPT and DFT-SAPT yield nearly identical results. Moreover, we are only interested in the relative trends in the interaction energies and therefore we believe that the DFT-SAPT results would be quite reliable.

It can be seen from Figure 2, that the close approach of the Cl^- to the $\pi\cdots Na^+$ and the $\pi\cdots NH_4^+$ complex leads to an increase in the magnitude of both the electrostatic and induction

TABLE 3: MP2/6-31+G* Charges of All the $M^+\cdots C_6H_6\cdots X^-$ Complexes[a]

	Li^+			Na^+			K^+			NH_4^+		
	F^-	Cl^-	Br^-	F^-	Cl^-	Br^-	F^-	Cl^-	Br^-	F^-	Cl^-	Br^-
M^+	0.91	0.92	0.92	0.94	0.95	0.95	0.98	0.98	0.98	0.90	0.91	0.91
C_6H_6	0.07	0.05	0.04	0.04	0.02	0.01	0.01	0.00	−0.01	0.08	0.06	0.06
X^-	−0.98	−0.97	−0.96	−0.98	−0.97	−0.96	−0.99	−0.98	−0.97	−0.98	−0.97	−0.97

[a] The charges (au) have been obtained using the natural bond orbital methodology and the MP2 densities. For the sake of brevity, only the net charge of the aromatic system is listed.

TABLE 4: MP2 Equivalent SAPT Interaction Energies of Several Representative $(M^+-C_6H_6)\cdots X^-$ Complexes and Their Subcomplexes Evaluated Using the 6-31G* Basis Set[a]

	Na^+			Cl^-		
	F^-	Cl^-	Br^-	Li^+	K^+	NH_4^+
			$E_{(M^+-\pi)\cdots X^-}$			
E_{int}	−73.92	−65.30	−64.40	−72.59	−57.81	−57.08
E_{es}	−94.36	−76.25	−75.89	−85.23	−67.98	−67.53
E_{exch}	68.68	44.71	52.96	49.94	40.88	40.51
E_{ind}	−40.84	−27.36	−32.89	−30.41	−24.78	−24.25
E_{disp}	−7.40	−6.40	−8.59	−6.89	−5.93	−5.81
			$E_{p\cdots X^-}$			
E_{int}	9.07	6.86	6.20	7.50	6.56	8.40
E_{es}	−11.61	−4.52	−5.93	−5.38	−3.73	−2.29
E_{exch}	65.12	41.66	49.26	45.76	38.17	37.75
E_{ind}	−36.79	−23.66	−28.25	−25.67	−21.81	−21.13
E_{disp}	−7.66	−6.62	−8.89	−7.20	−6.07	−5.93
			$E_{M^+\cdots X^-}$			
E_{int}	−75.64	−65.66	−64.87	−73.47	−59.47	−59.22
E_{es}	−74.81	−64.59	−63.26	−71.66	−58.77	−58.48
E_{exch}	−0.04	−0.23	−0.41	−0.57	−0.06	−0.07
E_{ind}	−0.78	−0.83	−1.20	−1.24	−0.62	−0.65
E_{disp}	0.00	0.00	−0.01	0.00	−0.02	−0.03

[a] All energies are in kcal/mol. All the calculations for the subcomplexes were carried out at the optimized geometries of the corresponding ternary complexes.

TABLE 5: MP2 Equivalent SAPT Interaction Energies of Several Representative $(M^+-C_6H_6)\cdots X^-$ Complexes and Their Subcomplexes Evaluated Using the 6-31G* Basis Set[a]

	Cl^-			Na^+		
	Li^+	K^+	NH_4^+	F^-	Cl^-	Br^-
			$E_{M^+\cdots(\pi-X)}$			
E_{int}	−117.69	−80.96	−83.14	−107.73	−96.88	−95.40
E_{es}	−102.28	−85.04	−84.88	−108.93	−95.91	−93.91
E_{exch}	23.02	35.23	29.10	40.20	34.89	34.50
E_{ind}	−37.90	−28.25	−21.53	−38.21	−35.11	−35.25
E_{disp}	−0.53	−2.89	−5.84	−0.79	−0.75	−0.74
			$E_{\pi\cdots M^+}$			
E_{int}	−37.40	−16.27	−17.52	−24.53	−24.50	−24.61
E_{es}	−21.92	−18.30	−19.16	−22.54	−21.78	−21.73
E_{exch}	18.94	24.87	23.95	27.79	26.32	25.86
E_{ind}	−33.92	−20.13	−16.89	−29.06	−28.34	−28.05
E_{disp}	−0.50	−2.71	−5.42	−0.72	−0.69	−0.69

[a] All energies are in kcal/mol. All the calculations for the subcomplexes were carried out at the optimized geometries of the corresponding ternary complexes.

energies. But, as can be noted from the slopes, this increase is more pronounced in the case of the induction energies. A similar observation can be made when the cations approach the corresponding $\pi\cdots Cl^-$ complex. What, however, distinguishes the approach of the cation and the anion is the trends of the total interaction energy around the equilibrium geometry. In the case of the anion approaching the cation−π complex, the total interaction energy is nearly flat. However, in the case of the cation approaching the anion−π complex, the total interaction energy becomes very repulsive as the cation comes very close. Though the above data can also be rationalized from the larger

TABLE 6: SAPT Decomposition of the Binding Energy (kcal/mol) of the $NH_4^+\cdots(C_6H_6\cdots Cl^-)$ Complex and Its Subcomplexes at the MP2/aug-cc-pVDZ Level[a]

	E_{int}	E_{es}	E_{ind}	E_{disp}	E_{exch}
$E_{M^+\cdots X^-}$	−59.86	−58.85	−0.90	−0.06	0.05
$E_{M^+\cdots\pi}$	−18.54	−17.56	−22.29	−9.94	36.32
$E_{\pi\cdots X^-}$	3.60	−5.41	−24.54	−13.23	46.41
ΣE_{ij}	−74.80	−81.81	−47.73	−23.23	82.77
$E_{M^+\cdots(\pi\cdots X^-)}$	−87.60	−86.55	−27.81	−10.82	44.51
$\delta E_{(\pi\cdots X^-)}$	−9.20	−10.14	−4.62	−0.83	8.14
$E_{(M^+\cdots\pi)\cdots X^-}$	−65.42	−73.03	−27.50	−12.77	48.14
$\delta E_{(M^+\cdots\pi)}$	−9.16	−8.78	−2.06	0.52	1.68
$E_{(M^+\cdots X^-)\cdots\pi}$	−25.64	−31.70	−80.57	−25.74	117.18
$\delta E_{(M^+\cdots X^-)}$	−10.70	−8.73	−33.73	−2.57	34.45

[a] All energies are in kcal/mol. All the calculations for the subcomplexes were carried out at the optimized geometries of the corresponding ternary complexes.

$R_{\pi\cdots X^-}$ intermolecular distance as compared to $R_{M^+\cdots\pi}$ in the equilibrium geometry, we believe that this observation indicates that the presence of counterions (anions) plays an important role in enhancing the large induction-driven energy of the cation−π interaction.

These changes in the interaction energies can also be visualized in terms of the electron-density redistribution upon the formation of the ternary complex. In Figure 3, the electron density difference distribution of the $Na^+\cdots\pi$, $Cl^-\cdots\pi$, and $Na^+\cdots\pi\cdots Cl^-$ complexes are shown. It can be seen that the formation of the ternary complex is associated with an increase in the electron density in the region between the Na^+ and benzene and a decrease in the electron density in the region between the benzene and Cl^-. The presence of both the cation and anion on opposite sides of the benzene π electron cloud leads to a strongly polarized reorganization of the π electron density. This brings the anion closer to the π system and thereby leads to an enhanced binding energy gain. A similar conclusion can be made from Figure 4, wherein the electron density difference distribution of the $NH_4^+\cdots\pi\cdots Cl^-$ is depicted.

4. Conclusions

Given the current interest in the properties of weak noncovalent interactions, the present theoretical investigation examines the effects of the simultaneous interaction of a cation and an anion with a π system. In the course of this study, we have carried out a detailed analysis of the interaction energies, which include evaluation of the two-body, three-body contributions as well as the magnitudes of the individual energy components (electrostatic energy, induction, dispersion and exchange repulsion) constituting the total interaction energy. The following conclusions can be made from this study. (i) In the gas phase, the benzene−cation−anion complex would be the most stable, and the charge transfer (either small or large) would reduce the cationic charge, resulting in reducing the cation−π interaction. Namely, when an ion-pair contact is formed, the cation−π interaction would be significantly reduced.[18] (ii) On the other hand, in the cases when the cation and anion are on the opposite

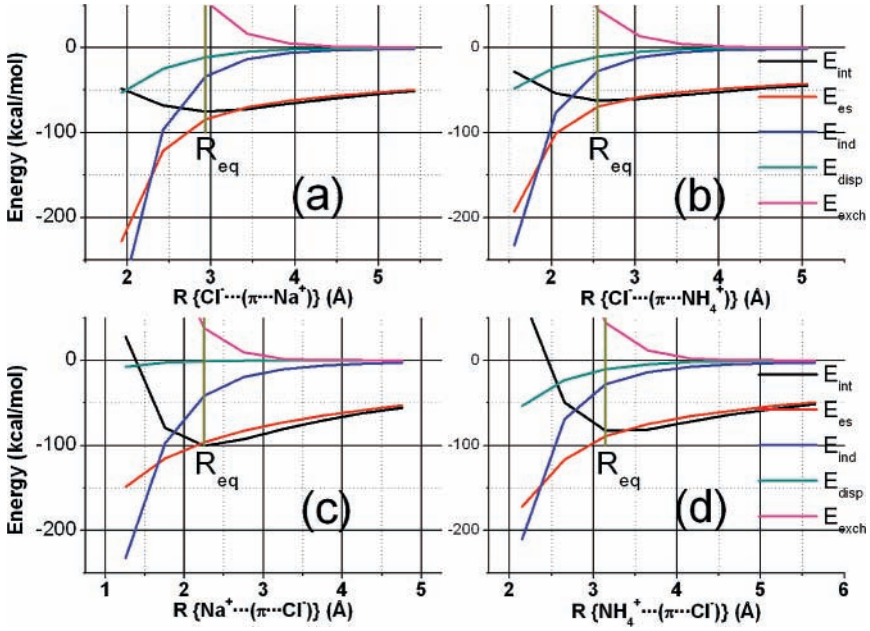

Figure 2. Modulation of all the intermolecular interaction energy components (E_{int}, E_{es}, E_{in}, E_{disp}, E_{exch}) upon bringing the anion (Cl^-) (a, b) or the cations (Na^+ or NH_4^+) (c, d) close to the corresponding ($\pi\cdots Na^+$), ($\pi\cdots NH_4^+$), or ($\pi\cdots Cl^-$) systems.

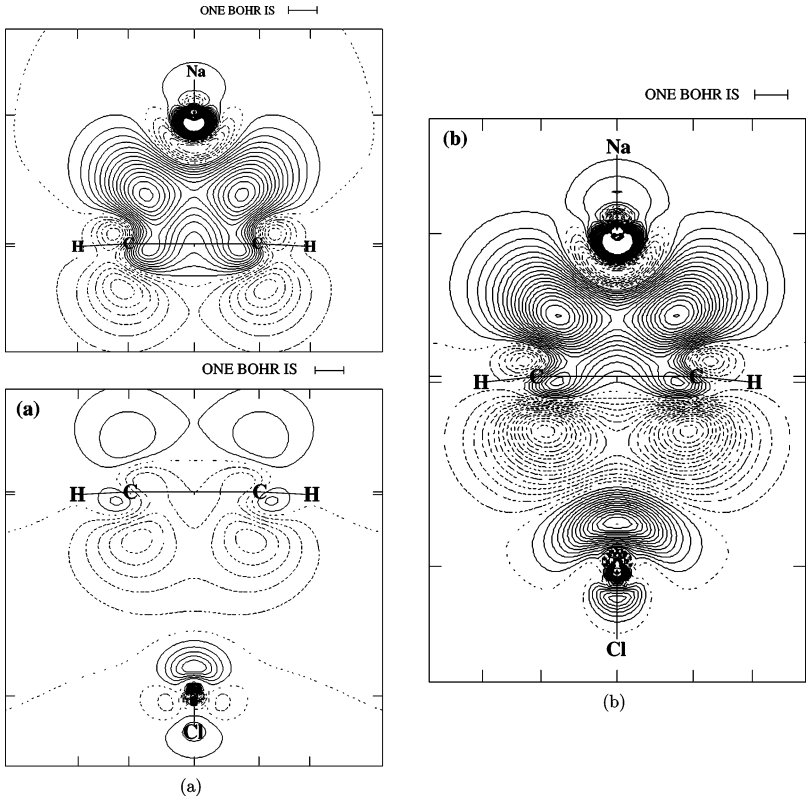

Figure 3. Contour line diagram of the difference of electron density distribution of the $Na^+\cdots\pi$, $Cl^-\cdots\pi$, and $Na^+\cdots\pi\cdots Cl^-$ complexes. Contour lines range from 1×10^{-6} to 1×10^{-2} [e/bohr^3]. Solid lines correspond to an increase of electron density upon complex formation, and dashed lines to a decrease.

sides of the π system, the induction effect is strongly enhanced and existence of a cation can enable the binding of π with an anion. Thus, in this case, the geometrical change in the $\pi-$anion distance is substantial.

This study yields valuable information in understanding crystal packing,[13−15] and also in the transport of ions in biological systems.[20] The dominant interactions of cation−benzene−anion complex, as seen in the well-studied Dougherty's cyclophane platform and ammonium cation channel are the cation−anion interaction and the cation−π interaction.[19,20] The presence of the anion enhances the complexation energy with the large induction effect, in agreement with the enhanced binding energy for a cation by the Dougherty receptor with carboxylic anions attached to the outside of aromatic rings.[19] This study also provides an explanation of the role played by the negatively charged amino acid (Asp160) residue in govern-

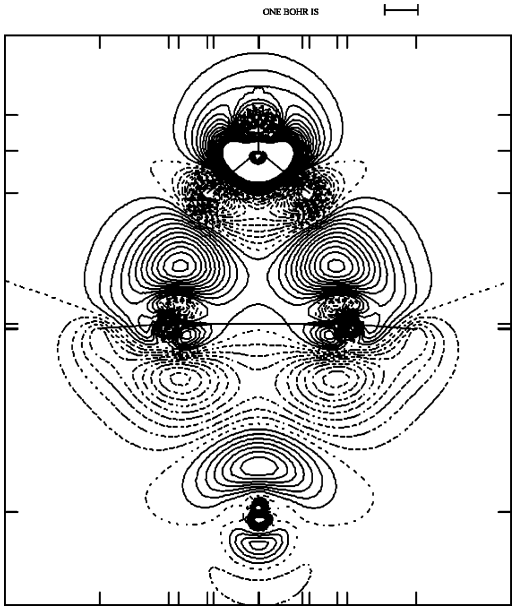

Figure 4. Contour line diagram of the difference of electron density distribution of the $NH_4^+\cdots\pi\cdots Cl^-$ complex. Contour lines range from 1×10^{-6} to 1×10^{-2} [e/bohr^3]. Solid lines correspond to an increase of electron density upon complex formation, and dashed lines to a decrease. NH_4^+, C_6H_6, and Cl^- are at the top, middle, and bottom of the figure, respectively.

ing the ammonium cation-attracting capabilities of the hydrophobic aromatic amino acid residues.[20]

Acknowledgment. This work was supported by the Global Research Laboratory Program of the Korean Ministry of Science and Technology. Partial support was also obtained from the Brain Korea 21 program of the Korean Ministry of Education.

References and Notes

(1) Lehn, J.-M. *Supramolecular Chemistry*; VCH: Weinheim, 1995.
(2) Aviram, A.; Ratner, M. A.; Mujica, V. *Ann. N. Y. Acad. Sci*. **2002**, *960*, 1. Aviram, A.; Ratner, M. A. *Ann. N. Y. Acad. Sci.* **2002**, *852*, 1.
(3) Yoon, J.; Kim, S. K.; Singh, N. J.; Kim, K. S. *Chem. Soc. Rev.* **2006**, *35*, 355.
(4) Meyer, E. A.; Castellano, R. K.; Diederich, F. *Angew. Chem., Int. Ed.* **2003**, *42*, 1210.
(5) Lopinski, G. P.; Wayner, D. D. M.; Wolkow, R. A. *Nature* **2000**, *406*, 48.
(6) Hong, B. H.; Lee, J. Y.; Lee, C.-W.; Kim, J. C.; Bae, S. C.; Kim, K. S. *J. Am. Chem. Soc.* **2001**, *123*, 10748.
(7) Kim, K. S.; Suh, S. B.; Kim, J. C.; Hong, B. H.; Lee, E. C.; Yun, S.; Tarakeshwar, P.; Lee, J. Y.; Kim, Y.; Ihm, H.; et al. *J. Am. Chem. Soc.* **2002**, *124*, 14268.
(8) Kim, H. G.; Lee, C.-W.; Yun, S.; Hong, B. H.; Kim, Y.-O.; Kim, D.; Ihm, H.; Lee, J. W.; Lee, E. C.; Tarakeshwar, P.; Park, S.-M.; Kim, K. S. *Org. Lett*. **2002**, *4*, 3971.
(9) Burley, S. K.; Petsko, G. A. *Science* **1985**, *229*, 23.
(10) Gazit, E. *FASEB J.* **2002**, *16*, 77.
(11) Lee, E. C.; Kim, D.; Jurecka, P.; Tarakeshwar, P.; Hobza, P.; Kim, K. S. *J. Phys. Chem. A* **2007**, *111*, 3446.
(12) Izzat, R. M.; Pawlak, K.; Bradshaw, J. S.; Bruening, R. L. *Chem. Rev.* **1991**, *91*, 1721. Izzat, R. M.; Pawlak, K.; Bradshaw, J. S.; Bruening, R. L. *Chem. Rev.* **1995**, *95*, 2529. Islam, M. S.; Pethrick, R. A.; Pugh, D.; Wilson, M. J. *J. Chem. Soc. Faraday Trans.* **1998**, *94*, 39.
(13) Nathanson, G. M.; Davidovits, P.; Worsnop, D. R.; Kolb, C. E. *J. Phys. Chem.* **1996**, *100*, 13007. Laskin, A.; Gaspar, D. J.; Wang, W.-H.; Hunt, S. W.; Cowin, J. P.; Colson, S. D.; Finlayson-Pitts, B. J. *Science* **2003**, *301*, 340.
(14) MacGillivray, L. R.; Atwood, J. L. *J. Chem. Soc. Chem. Commun*. **1997**, 44. Bodkin, M. J.; Goodfellow, J. M. *Protein Sci.* **1995**, *4*, 603. Dill, K. A.; Fiebig, K. M.; Chan, H. S. *Proc. Natl. Acad. Sci*. U.S.A. **1993**, *90*, 1942.
(15) King, B. T.; Noll, B. C.; Michl, J. *Collect. Czech. Chem. Commun*. **1999**, *64*, 1001.
(16) Garau, C.; Quiñonero, D.; Frontera, A.; Ballester, P.; Costa, A.; Deyá, P. M. *New J. Chem.* **2003**, *27*, 211.
(17) Bartoli, S.; Roelens, S. *J. Am. Chem. Soc.* **2002**, *124*, 8307.
(18) Per-Ola, N.; Liljefors, T. *J. Am. Chem. Soc.* **1999**, *121*, 2303.
(19) Ngola, S. M.; Kearney, P. C.; Mecozzi, S.; Russell, K.; Dougherty, D. A. *J. Am. Chem. Soc.* **1999**, *121*, 1192.
(20) Khademi, S.; O'Connell, J., III; Remis, J.; Robles-Colmenares, Y.; Miercke, L. J. W.; Stroud, R. M. *Science* **2004**, *305*, 1587.
(21) Kim, K. S.; Tarakeshwar, P.; Lee, J. Y. *Chem. Rev.* **2000**, *100*, 4145.
(22) Ma, J. C.; Dougherty, D. A. *Chem. Rev.* **1997**, *97*, 1303.
(23) Gokel, G. W.; Mukhopadhyay, A. *Chem. Soc. Rev.* **2001**, *30*, 274. Gokel, G. W.; De Wall, S. L.; Meadows, E. S. *Eur. J. Org. Chem.* **2000**, 2967.
(24) Kim, D.; Hu, S.; Tarakeshwar, P.; Kim, K. S.; Lisy, J. M. *J. Phys. Chem. A* **2003**, *107*, 1228.
(25) Kim, D.; Tarakeshwar, P.; Kim, K. S. *J. Phys. Chem. A* **2004**, *108*, 1250.
(26) Beer, P. D.; Gale, P. A. *Angew. Chem., Int. Ed.* **2001**, *40*, 486.
(27) Hankins, D.; Moskowitz, J. W.; Stillinger, F. H. *J. Chem. Phys.* **1970**, *53*, 4544.
(28) Kim, K. S.; Dupuis, M.; Lie, G. C.; Clementi, E. *Chem. Phys. Lett.* **1986**, *131*, 451.
(29) Mhin, B. J.; Kim, J.; Lee, S.; Lee, J. Y.; Kim, K. S. *J. Chem. Phys.* **1994**, *100*, 4484.
(30) Kim, J.; Lee, S.; Cho, S. J.; Mhin, B. J.; Kim, K. S. *J. Chem. Phys.* **1995**, *102*, 839.
(31) Jeziorski, B.; Szalewicz, K. In *Encyclopedia of Computational Chemistry*; Schleyer, P. v. R., Allinger, N. L., Clark, T., Gasteiger, J., Kollman, P. A., Schaefer, H. F., III, Schreiner, P. R., Eds.; Wiley: Chichester, U.K., 1998.
(32) Jeziorski, B.; Moszynski, R.; Szalewicz, K. *Chem. Rev.* **1994**, *94*, 1887. Szalewicz, K.; Jeziorski, B. In *Molecular Interactions - From van der Waals to Strongly Bound Complexes*; Scheiner, S., Ed.; Wiley: New York, 1997; p 3.
(33) Jeziorski, B.; Moszyński, R.; Ratkiewicz, A.; Rybak, S.; Szalewicz, K.; Williams, H. L. In *Methods and Techniques in Computational Chemistry: METECC-94, Vol. B, Medium Sized Systems*; Clementi, E., Ed.; STEF: Cagliari, 1993; pp 79−129.
(34) Kraka, E.; Cremer, D.; Spoerel, U.; Merke, I.; Stahl, W.; Dreizler, H. *J. Phys. Chem.* **1995**, *99*, 12466.
(35) Spoerel, U.; Dreizler, H.; Stahl, W.; Kraka, E.; Cremer, D. *J. Phys. Chem.* **1996**, *100*, 14298.
(36) Oh, J. J.; Park, I.; Wilson, R. J.; Peebles, S. A.; Kuczkowski, R. L.; Kraka, E.; Cremer, D. *J. Chem. Phys.* **2000**, *113*, 9051.
(37) Tarakeshwar, P.; Kim, K. S.; Kraka, E.; Cremer, D. *J. Chem. Phys.* **2001**, *115*, 6018.
(38) Chalasiński, G.; Szczęśniak, M. M. *Chem. Rev.* **1994**, *94*, 1723. Chalasiński, G.; Szczęśniak, M. M. *Chem. Rev.* **2000**, *100*, 4227.
(39) Boys, S. F.; Bernardi, F. *Mol. Phys.* **1970**, *19*, 553.
(40) Reed, A. E.; Curtiss, L. A.; Weinhold, F. *Chem. Rev.* **1988**, *88*, 889.
(41) Frisch, M. J.; Trucks, G. W.; Schlegel, H. B.; Scuseria, G. E.; Robb, M. A.; Cheeseman, J. R.; Zakrzewski, J. A.; Montgomery, J. A.; Stratmann, R. E.; Burant, J. C.; Dapprich, S.; Millam, J. M.; Daniels, A. D.; Kudin, K. N.; Strain, M. C.; Farkas, O.; Tomasi, J.; Barone, V.; Cossi, M.; Cammi, R.; Mennucci, B.; Pomelli, C.; Adamo, C.; Clifford, S.; Ochterski, J.; Petersson, G. A.; Ayala, P. Y.; Cui, Q.; Morokuma, K.; Malick, D. K.; Rabuck, A. D.; Raghavachari, K.; Foresman, J. B.; Cioslowki, J.; Ortiz, J. V.; Stefanov, B. B.; Liu, G.; Liashenko, A.; Piskorz, P.; Komaromi, I.; Gomperts, R.; Martin, R. L.; Fox, D. J.; Keith, T.; Al-Laham, M. A.; Peng, C. Y.; Nanayakkara, A.; Gonzalez, C.; Challacombe, M.; Gill, P. M. W.; Johnson, B. G.; Chen, W.; Wong, M. W.; Andres, J. L.; Head-Gordon, M.; Replogle, E. S.; Pople, J. A. *Gaussian 98*, revision A.1; Gaussian, Inc.: Pittsburgh, PA, 1998.
(42) Schmidt, M. W.; Baldridge, K. K.; Boatz, J. A.; Elbert, S. T.; Gordon, M. S.; Jensen, J. H.; Koseki, S.; Matsunaga, N.; Nguyen, K. A.; Su, S. J.; Windus, T. L.; Dupuis, M.; Montgomery, J. A. *J. Comput. Chem.* **1993**, *14*, 1347.
(43) Tarakeshwar, P.; Choi, H. S.; Lee, S. J.; Lee, J. Y.; Kim, K. S.; Ha, T.-K, Jang, J. H.; Lee, J. G.; Lee, H. *J. Chem. Phys.* **1999**, *111*, 5838.
(44) Tarakeshwar, P.; Choi, H. S.; Kim, K. S. *J. Am. Chem. Soc.* **2001**, *123*, 3323.
(45) Tarakeshwar, P.; Kim, K. S.; Brutschy, B. *J. Chem. Phys.* **2000**, *112*, 1769. Tarakeshwar, P.; Kim, K. S.; Brutschy, B. *J. Chem. Phys.* **2001**, *114*, 1295.
(46) Bukowski, R.; Szalewicz, K.; Chabalowski, C. *J. Phys. Chem. A* **1999**, *103*, 7322.
(47) Milet, A.; Moszynski, R.; Wormer, P. E. S.; van der Avoird, A. *J. Phys. Chem. A* **1999**, *103*, 6811.
(48) Visentin, T.; Kochanski, E.; Moszynski, R.; Dedieu, A. *J. Phys. Chem. A* **2001**, *105*, 2023. Visentin, T.; Kochanski, E.; Moszynski, R.; Dedieu, A. *J. Phys. Chem. A* **2001**, *105*, 2031.
(49) Vaupel, S.; Brutschy, B.; Tarakeshwar, P.; Kim, K. *J. Am. Chem. Soc.* **2006**, *128*, 5416.

(50) Jansen, G.; Hesselmann, A. *J. Phys. Chem. A* **2001**, *105*, 11156; Jansen, G.; Hesselmann, A. *Chem. Phys. Lett.* **2003**, *367*, 778; Jansen, G.; Hesselmann, A.; Schütz, M. *J. Chem. Phys.* **2005**, *122*, 014103; Werner, H.-J.; Knowles, P. J.; Amos, R. D.; Bernhardsson, A.; Berning, A.; Celani, P.; Cooper, D. L.; Deegan, M. J. O.; Dobbyn, A. J.; Eckert, F.; Hampel, C.; Hetzer, G.; Knowles, P. J.; Korona, T.; Lindh, R.; Lloyd, A. W.; McNicholas, S. J.; Manby, F. R.; Meyer, W.; Mura, M. E.; Nicklass, A.; Palmieri, P.; Pitzer, R.; Rauhut, G.; Schütz, M.; Schumann, U.; Stoll, H.; Stone, A. J.; Tarroni, R.; Thorsteinsson, T.; Werner, H.-J. *MOLPRO*, version 2006.1.